Photoinduced electron transfer in a triarylamine-organoboron-Ru(2,2'-bipyridine)$_3^{2+}$ compound

Luisa G. Heinz and Oliver S. Wenger*

Department of Chemistry, University of Basel, St. Johanns-Ring 19, 4056 Basel, Switzerland

Email: oliver.wenger@unibas.ch

Abstract

Long-range electron transfer reactions play a key role in biological photosynthesis, and they are likely to play an important role for future artificial photosynthetic endeavors as well. The possibility to control the rates for long-range electron transfer with external stimuli is of particular interest in this context. In the work presented herein, we explored a donor-bridge-acceptor compound in which intramolecular electron transfer from a triarylamine donor to a photoexcited Ru(bpy)$_3^{2+}$ (bpy = 2,2'-bipyridine) acceptor occurs across an organoboron bridge over a distance of approximately 22 Å. Fluoride has a high binding affinity to the organoboron bridge in apolar solution, and the resulting organofluoroborate has a significantly different electronic structure. We explored to what extent the change from an electron-deficient organoboron wire to an electron-rich organofluoroborate bridge affects long-range electron transfer between the distant triarylamine donor and the Ru(bpy)$_3^{2+}$ acceptor.

Keywords

Electron transfer, time-resolved spectroscopy, donor-acceptor systems, photochemistry, voltammetry, ruthenium

1. Introduction

Organoboron compounds have received significant attention in recent years as (fluoride) sensor materials [1-3], for opto-electronic applications [4-6], and for fundamental studies of charge transfer phenomena [7-9]. In the vast majority of these charge transfer studies, the boron center acted as a terminal electron acceptor, but the efficiency of organoboron compounds as molecular bridges (or "wires") between a donor and a more potent acceptor has not been investigated until very recently. In a study published in 2015, we demonstrated that intramolecular electron transfer between the triarylamine unit and photoexcited $Ru(bpy)_3^{2+}$ (bpy = 2,2'-bipyridine) across the organoboron bridge of the dyad in Scheme 1a can be controlled by fluoride anions [10]. Specifically, in absence of F^- intramolecular electron transfer occurred with a rate constant (k_{ET}) $\geq 10^8$ s^{-1}, but when two fluoride anions were bound to the organoboron bridge, k_{ET} decreased to $\leq 10^6$ s^{-1}. Here, we present results that we obtained on the structurally similar **TAA-B-Ru^{2+}** dyad shown in Scheme 1b. We were curious to explore whether the *meta*-linkage in the new dyad permits an equally efficient switching of long-range electron transfer as in our previously studied dyad.

The possibility to control the rates of long-range electron transfer is of interest in the greater contexts of a future molecular electronics technology and artificial photosynthesis.

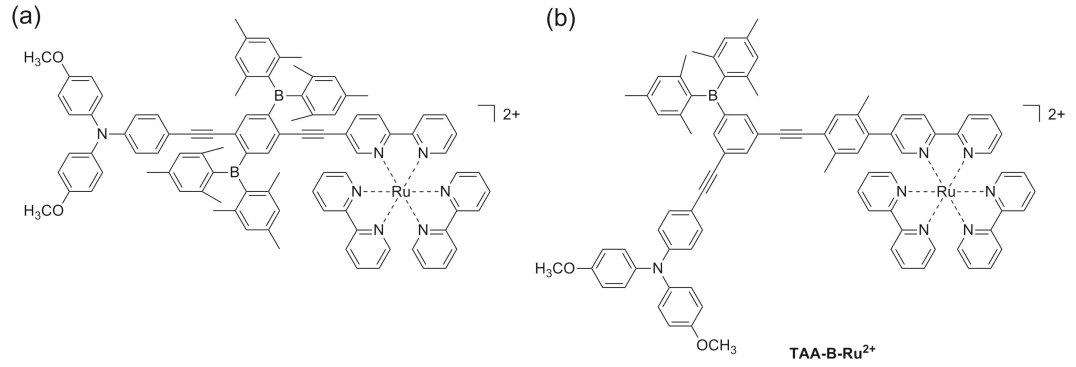

Scheme 1. Chemical structures of two triarylamine-organoboron-$Ru(bpy)_3^{2+}$ compounds: (a) Previously studied system [10]; (b) new system presented herein.

2. Results and discussion

2.1 Synthesis

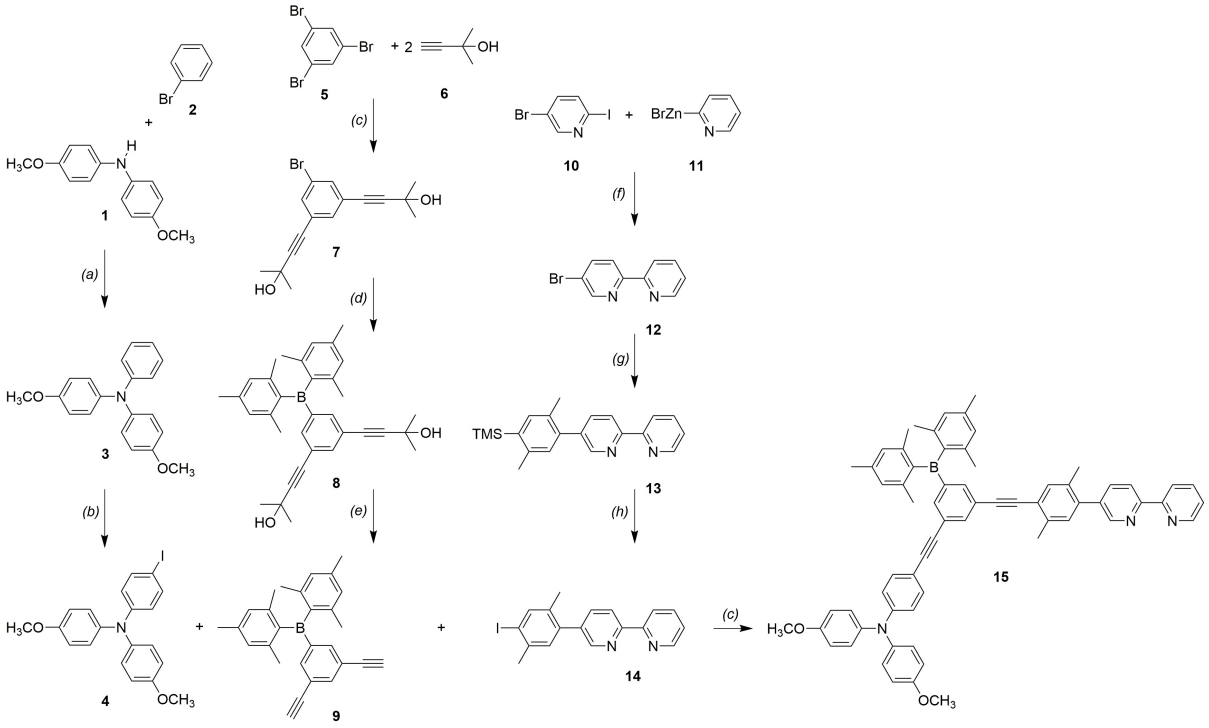

Scheme 2. Synthesis of the key ligand for the **TAA-B-Ru**$^{2+}$ dyad from Scheme 1b: (a) P(^{t}Bu)$_3$H$^+$BF$_4^-$, Pd(dba)$_2$, ^{t}BuOK, toluene; (b) $C_6H_5I(CF_3COO)_2$, I_2, CH_2Cl_2; (c) Et_3N , CuI, $PdCl_2(PPh_3)_2$; (d) *n*-BuLi, $Bmes_2F$, Et_2O; (e) NaH, toluene; (f) $Pd(PPh_3)_4$, THF [11]; (g) 2,5-dimethyl-4-trimethylsilyl-1-phenylboronic acid [12, 13], $Pd(PPh_3)_4$, Na_2CO_3, THF/H_2O; (h) ICl, CH_3CN/CH_2Cl_2.

The synthesis of the key ligand of the **TAA-B-Ru**$^{2+}$ compound is illustrated in Scheme 2. The triarylamine donor moiety was introduced into the **TAA-B-Ru**$^{2+}$ dyad using the iodo-substituted triarylamine compound **4** which was prepared following previously published protocols [14, 15]. The dimesitylboron-substituted bridging unit was prepared starting from 1,3,5-tribromobenzene (**5**) which was reacted with 2 equivalents of 2-methyl-3-butyn-2-ol (**6**) to afford compound **7** [16]. The latter was reacted with dimesitylfluoroborane in order to obtain compound **8**. Subsequent deprotection with NaH gave the dialkynyl compound **9**. The iodo-xylene substituted bpy ligand unit **14** was prepared

following our own published protocols [11, 15]. Ligand **15** was obtained by reacting triarylamine compound **4**, dimesitylboron-substituted bridging unit **9**, and bpy ligand unit **14** in 1:1:1 molar ratio using standard Sonogashira coupling conditions. Subsequent reaction with $Ru(bpy)_2Cl_2$ afforded the **TAA-B-Ru^{2+}** dyad.

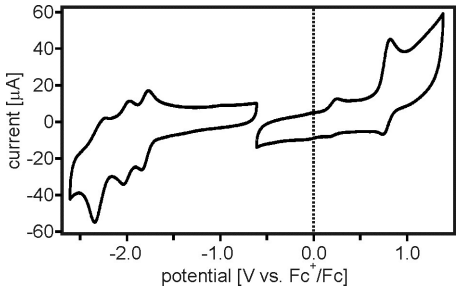

Figure 1. Cyclic voltammograms of the **TAA-B-Ru^{2+}** dyad in CH_3CN measured in presence of 0.1 M $TBAPF_6$. Oxidative and reductive potential sweeps with rates of 0.1 V/s were performed separately because this gave higher quality results.

2.2 Electrochemistry

Cyclic voltammetry of the **TAA-B-Ru^{2+}** dyad was performed in CH_3CN containing 0.1 M $TBAPF_6$ as a supporting electrolyte. Oxidative and reductive potential sweeps with rates of 0.1 V/s were conducted separately because this gave higher quality results. Typical scans are shown in Figure 1. Oxidation of the triarylamine unit is detected at 0.20 V vs. $Fc^{+/0}$ and oxidation of Ru(II) occurs at 0.77 V vs. $Fc^{+/0}$, both in line with expectation [10, 17, 18]. Based on prior studies,[18] we expect that the Ru(II/III) wave overlaps with the wave associated with oxidation of the triarylamine monocation to its dicationic form. The latter is unstable and can undergo carbazole formation. This explains both the poor reversibility of the wave at 0.20 V vs. $Fc^{+/0}$ and the significantly stronger current associated with the wave at 0.77 V vs. $Fc^{+/0}$.

Compared to the previously investigated compound from Scheme 1a, oxidation of the ruthenium center in **TAA-B-Ru^{2+}** is approximately 0.33 V easier to perform. Presumably this is due to the fact

that in the new system the $Ru(bpy)_3^{2+}$ unit is electronically more decoupled from the electron-deficient organoboron unit by the additional *p*-xylene spacer.

In the reductive sweep, one recognizes three quasi-reversible reduction waves which are attributed to consecutive one-electron reduction of each of the three bpy ligands. Reduction of the boryl bridging unit would be expected to occur at ca. -2.2 V vs. $Fc^{+/0}$ based previously reported values for comparable compounds [7, 10, 19-23], but in Figure 1 the respective reduction cannot be observed unambiguously; we suspect that it is overlapped by one of the bpy-related reduction waves.

Given an energy (E_{00}) of 2.1 eV for the emissive ^{3}MLCT excited state of the $Ru(bpy)_3^{2+}$ unit and a distance (R_{DA}) of ~22 Å between the triarylamine N atom and the Ru(II) center in the **TAA-B-Ru^{2+}** dyad [24], the redox potentials (E^0) from Table 1 can be used to estimate the reaction free energy (ΔG_{ET}^0) for intramolecular electron transfer from TAA to the photoexcited ruthenium complex [25].

$$\Delta G_{ET}^0 = e\cdot(E^0(TAA^{+/0}) - E^0(bpy^{0/-})) - E_{00} - e^2 / (4\cdot\pi\cdot\varepsilon_0\cdot\varepsilon_s\cdot R_{DA}) \quad \text{(eq. 1)}$$

Photoinduced electron transfer leads to oxidation of the triarylamine unit, hence the use of its oxidation potential in equation 1. The reduction product is $Ru(bpy)_3^+$, with the additional electron hosted by a bpy-localized orbital hence the use of the first bpy reduction potential in equation 1. Photoexcitation is taken into account by the E_{00} term which represents the ^{3}MLCT energy of the $Ru(bpy)_3^{2+}$ sensitizer. Equation 1 yields ΔG_{ET}^0 = -0.2 eV which leads to the expectation of photoinduced electron transfer upon excitation of the $Ru(bpy)_3^{2+}$ unit of **TAA-B-Ru^{2+}**. This driving-force is similar to that previously determined for the dyad from Scheme 1a (ΔG_{ET}^0 = -0.3 eV).

Table 1. Reduction potentials (in Volts vs. Fc^+/Fc) of the individual sub-components of the **TAA-B-Ru^{2+}** dyad in CH_3CN.[a]

	E^0 [V]
$TAA^{+/0}$	0.20

$Ru^{III/II}$	0.77
$bpy^{0/-}$	-1.82
$bpy^{0/-}$	-2.00
$bpy^{0/-}$	-2.29
$boryl^{0/-}$	-2.20[b]

[a] Extracted from Figure 1; [b] from ref. [10].

Attempts to perform cyclic voltammetry in CH_2Cl_2 were unsuccessful, the resulting data quality was very poor.

2.3 UV-Vis absorption and F^- binding

The optical absorption spectrum of a 10^{-5} M solution of **TAA-B-Ru^{2+}** in CH_2Cl_2 is shown in Figure 2 (solid line). The ^{1}MLCT absorption band of the $Ru(bpy)_3^{2+}$ unit is the lowest-energy absorption feature with a maximum at 460 nm. At 350 nm there is an absorption feature that can be attributed to a N → B charge transfer band, as commonly observed in triarylamine-triarylboron compounds [4, 6-8, 26-30]. At 290 nm one detects bpy-localized π-π* absorptions.

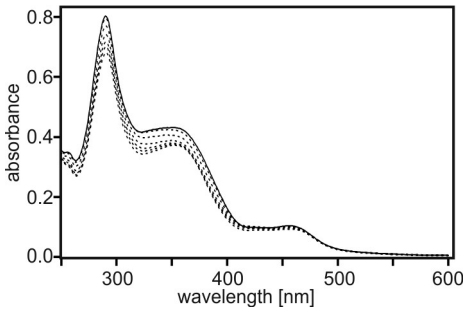

Figure 2. Solid trace: UV-Vis spectrum of 10^{-5} M **TAA-B-Ru^{2+}** in CH_2Cl_2 at 22 °C. Dashed traces: Spectra measured from the same solution upon addition of increasing amounts of TBAF.

Upon addition of TBAF, the N → B charge transfer absorption decreases (dotted lines), as expected when F^- binding suppresses optical charge transfer [7, 26]. This kind of observation forms the basis for many fluoride detectors [1, 26, 31]. In Figure 3 the absorbance at 370 nm is plotted as a function of F^- concentration. This titration curve is based on the solution from Figure 2 which has a nominal **TAA-B-Ru^{2+}** concentration of 10^{-5} M. Given the presence of one boron atom on the bridging unit of **TAA-B-Ru^{2+}**, one expects 1:1 association between F^- and **TAA-B-Ru^{2+}** [1, 2]. Consequently, the data in Figure 3 was analyzed within the framework of a 1:1 binding model to extract an association constant (K_A) between F^- and the boron center (equation 2) [32-34].

$$A(c_F) = A_0 + [(A_{lim} - A_0) / 2 \cdot c_0] \cdot [c_0 + c_F + K_A^{-1} - [(c_0 + c_F + K_A^{-1})^2 - 4 \cdot c_0 \cdot c_F]^{1/2}] \quad \text{(eq. 2)}$$

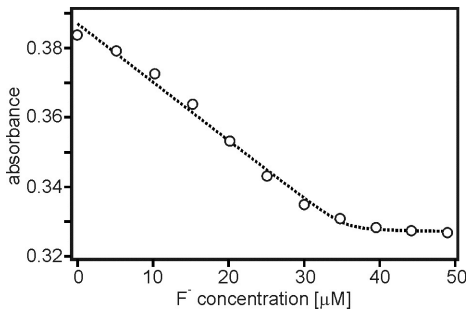

Figure 3. Titration curve based on the data in Figure 2, displaying the absorbance at 370 nm as a function of fluoride concentration.

In equation 2, $A(c_F)$ is the absorbance of the sample as a function of F^- concentration, and A_0 is the absorbance of the initial analyte solution prior to addition of any titrant. A_{lim} is the limiting absorbance value which is obtained in presence of a large excess of titrant, c_0 is the concentration of the analyte (**TAA-B-Ru^{2+}**). The dotted line in Figure 3 is the result of a fit with equation 2 to the experimental data, yielding $K_A = (1.7\pm0.5)\cdot10^7$ M^{-1}, $A_0 = 0.387$, $A_{lim} = 0.327$, $c_0 = (3.5\pm1.4)\cdot10^{-5}$ M. The latter had to be a freely adjustable parameter for successful fitting with this binding model. Of key interest here is the apparent association constant, which is in reasonable agreement with fluoride binding studies of chemically related organoboron compounds in similarly apolar solution [1, 2, 7, 32, 35, 36]. It should be kept in mind that trace amounts of water can strongly affect fluoride binding due to the high hydration enthalpy of F^-.

2.4 Transient absorption spectroscopy and spectro-electrochemistry

Following excitation of the **TAA-B-Ru^{2+}** dyad in CH_2Cl_2 (10^{-4} M) with laser pulses of 532 nm wavelength and ~10 ns duration, the transient absorption spectrum shown in Figure 4a (black trace) was obtained by time-integrating over a period of 40 ns immediately after the pulses. This spectrum exhibits absorption bands at 420, 540, and 730 nm, in addition to the (weak) bleach at 470 nm. All four of these spectral features can be understood on the basis of the spectro-electrochemical data in Figure 4b/c.

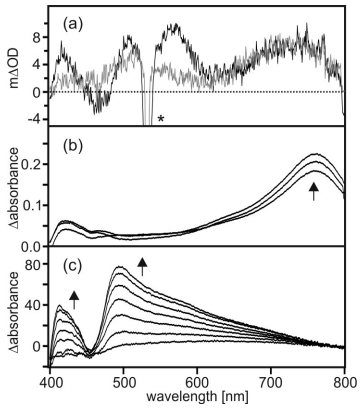

Figure 4. (a) Transient absorption spectra measured by time-integrating over a period of 40 ns following excitation at 532 nm with laser pulses of ~10 ns duration. Grey trace: 10^{-4} M **TAA-B-Ru^{2+}** in CH_2Cl_2. Red trace: 10^{-4} M **TAA-B-Ru^{2+}** in CH_2Cl_2 containing 2 equivalents of TBAF. (b) Spectro-electrochemistry showing the UV-Vis changes upon oxidation of TAA to TAA$^+$ in the **TAA-B-Ru^{2+}** dyad in CH_3CN. (c) Spectro-electrochemistry showing the UV-Vis changes upon reduction of $Ru(bpy)_3^{2+}$ to $Ru(bpy)_3^+$ in the **TAA-B-Ru^{2+}** dyad in CH_3CN.

For the series of UV-Vis difference spectra in Figure 4b, a potential sufficient for oxidation of the triarylamine unit of **TAA-B-Ru^{2+}** was applied to a Pt grid electrode (0.2 V vs. Fc^+/Fc). Absorption bands at 420 and 760 nm were detected, as expected [18]. When applying a potential sufficiently negative for bpy reduction (-1.5 V vs. Fc^+/Fc), the UV-Vis difference spectra shown in Figure 4c were measured. In this case, bands at 420 and 490 nm appear along with a bleach at 455 nm, compatible with one-electron reduction of the $Ru(bpy)_3^{2+}$ unit [37, 38]. In the spectro-electrochemical experiments of Figure 4b/c the UV-Vis spectrum of the **TAA-B-Ru^{2+}** dyad in CH_3CN prior to applying any electrochemical potential was used as a baseline, and therefore the resulting difference spectra can be directly compared to the transient absorption spectrum in Figure 4a (black trace). Based on this comparison we conclude that the photoproduct observed in the transient absorption spectrum contains oxidized triarylamine and reduced $Ru(bpy)_3^{2+}$. This is direct evidence for intramolecular photoinduced electron transfer, as expected based on the driving-force estimation made above (ΔG_{ET}^0 = -0.2 eV). In the following, the resulting photoproduct will be abbreviated as **TAA$^+$-B-Ru$^+$**.

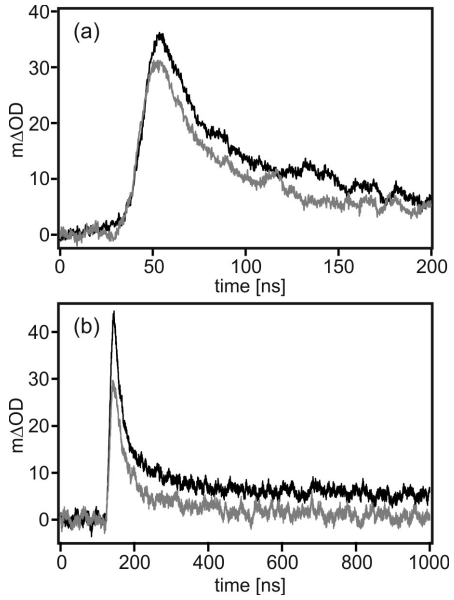

Figure 5. Temporal evolution of the transient absorption signals at 750 nm (from Figure 4a) on a short (a) and a longer timescale (b). Black trace: 10^{-4} M **TAA-B-Ru^{2+}** in CH_2Cl_2. Grey trace: 10^{-4} M **TAA-B-Ru^{2+}** in CH_2Cl_2 containing 2 equivalents of TBAF.

2.5 Electron transfer kinetics

In Figure 5 the temporal evolution of the transient absorption signal at 750 nm is shown (black traces). The risetime of the signal is instrumentally limited, indicating that formation of **TAA^+-B-Ru^+** occurs with a rate constant $k_{ET} \geq 10^8$ s^{-1}. The decay is tri-exponential with lifetimes of 20 ns, 135 ns, and >1000 ns. This rather complex decay behavior is most likely owed to the combination of reaction pathways involving intramolecular reverse electron transfer, bi-molecular electron transfer, and a degradation process.

When recording the transient absorption spectra with time delays ≥ 1000 ns, the typical spectroscopic signatures of TAA^+ and $Ru(bpy)_3^+$ cannot be detected any more. Consequently, the slowest time component of the tri-exponential decays is attributed to photo-degradation. The fastest time component (20 ns) is most likely the one associated with intramolecular reverse electron transfer across the covalent backbone of the **TAA-B-Ru^{2+}** dyad; for this process one expects comparatively strong electronic donor-acceptor coupling, and it seems plausible that this results in rapid electron transfer. The 135 ns time component is attributed to bimolecular processes. Due to the weakness of the transient absorption signals, relatively high sample concentrations (10^{-4} M) were used, and this increases the probability for intermolecular electron transfer significantly. Concentration dependence studies were not possible because the signals became undetectable upon dilution, and higher concentrations resulted in optical densities which were too elevated.

Thus we find that intramolecular reverse electron transfer occurs with a rate constant of $k_{rET} = 5 \cdot 10^7$ s^{-1}. Consequently, $k_{ET} > k_{rET}$, despite a significantly lower driving-force for photoinduced (forward) electron transfer (ΔG_{ET}^0 = -0.2 eV) compared to thermal (reverse) electron transfer (ΔG_{rET}^0 = -1.9 eV). The inverted driving-force effect is therefore likely at play [39], but there might also be differences in electronic coupling between forward and reverse electron transfer [40, 41].

2.6 Effect of F^- binding on electron transfer

The grey trace in Figure 4a is the transient absorption spectrum obtained for 10^{-4} M **TAA-B-Ru**$^{2+}$ in CH_2Cl_2 in presence of 2 equivalents of TBAF. The measurements conditions were identical as for the black trace in Figure 4a. While there are some spectral differences in the range from 400 to 620 nm between the measurements performed in absence (black) and presence of F^- (grey), the overall appearance of the spectra remains rather similar. Most importantly, the triarylamine cation band at 740 nm is clearly observed in both cases, and the spectral feature between 480 and 600 nm (attributed above to the reduced ruthenium complex) can still be detected. Thus one can conclude that photoinduced electron transfer does still occur when F^- is bound to the triarylboron bridging unit. The kinetics for **TAA**$^+$**-B-Ru**$^+$ photoproduct formation and disappearance are largely unaffected by fluoride binding (grey traces in Figure 5).

2.7 Comparison to a related organoboron dyad

In a recent study we investigated intramolecular electron transfer from the triarylamine unit to photoexcited $Ru(bpy)_3^{2+}$ in the dyad shown in Scheme 1a [10]. The key finding was that F^- binding to the organoboron bridging unit decreased k_{ET} from $\geq 10^8$ s^{-1} in absence of F^- to $\leq 10^6$ s^{-1} with two bound fluorides. Here we find that electron transfer across a similar bridge between the same donor and the same acceptor occurs with $k_{ET} \geq 10^8$ s^{-1}, regardless of whether F^- is bound or not. If any effect of F^- on the rate for photoinduced electron transfer is present at all, it has to affect the kinetics on a very rapid (<10 ns) timescale. Evidently, a deceleration of electron transfer to the microsecond time range does not occur. Aside from the presence of an additional *p*-xylene spacer in the dyad from Scheme 1b, the main differences between the compounds in Scheme 1a and Scheme 1b are the following: The bridging unit in the compound from Scheme 1b contains only one dimesitylboron-substituent which is in *meta*-position to the donor and acceptor units, whereas in the compound from Scheme 1a there are two dimesitylboron-groups which are in *ortho*- and *meta*-position to the donor and acceptor units. Electronic coupling between the *ortho*- and *para*-positions of benzene rings is known to be significantly stronger than electronic coupling between *meta*-positions [42-44]. Consequently, it can be argued that when F^- binds to the organoboron unit in the **TAA-B-Ru^{2+}** compound from Scheme 1b, this does not affect the electronic coupling pathway between the donor and the acceptor as much as in the case of the previously investigated dyad from Scheme 1a.

3. Summary and conclusions

Photoinduced electron transfer in the **TAA-B-Ru^{2+}** dyad from Scheme 1b occurs with a rate constant $k_{ET} \geq 10^8$ s^{-1} regardless of whether F^- is bound to the organoboron bridge or not. A deceleration of intramolecular electron transfer to rates on the microsecond timescale in presence of bound fluoride, such as previously observed for the dyad in Scheme 1a [10], is not detected for the new **TAA-B-Ru^{2+}**

compound. This contrasting behavior is attributed to the fact that the dimesitylboron unit of the **TAA-B-Ru^{2+}** dyad from Scheme 1b is electronically de-coupled from the donor-acceptor electron transfer pathway due to its attachment in *meta*-position. This strongly suggests that the k_{ET} switching observed for the dyad from Scheme 1a is mostly an electronic coupling effect rather than a simple electrostatic effect which arises from the binding of negative charges to the organoboron bridge.

4. Acknowledgements

This work was supported by the Deutsche Forschungsgemeinschaft (DFG) through grant number WE4815/3-1.

5. Experimental section

5.1 Materials and methods

Compounds **1**, **2**, **5**, **6**, **10** and **11** are commercial chemicals which were used as received. Compounds **3**, **4**, **12**, **13**, and **14** were synthesized according to our own previously published synthetic protocols [10, 15]. All other compounds were synthesized as described in the following.
Fluoride binding to the **TAA-B-Ru^{2+}** compound occurred by addition of commercial 1.0 M TBAF (tetra-*n*-butylammonium fluoride) solution in THF. Cyclic voltammetry was performed using a three-electrode setup comprised of a platinum disk working electrode, a silver wire as a counter electrode and a second silver wire as a quasi-reference electrode. A Versastat3-200 potentiostat from Princeton Applied Research was employed. Potential scans occurred with sweep rates of 0.1 V/s, $TBAPF_6$ (tetra-*n*-butylammonium hexafluorophosphate) was used as a supporting electrolyte in dry, de-aerated CH_3CN. A platinum grid working electrode was used for spectro-electrochemistry. NMR spectroscopy

was performed using a 400 MHz Bruker Avance III instrument. Mass spectra were recorded on a Bruker Esquire 3000 plus instrument. Elemental analysis was performed by Ms. Sylvie Mittelheisser in the Department of Chemistry at University of Basel using a Vario Micro Cube instrument from Elementar. UV-Vis absorption spectra were measured on a Cary 5000 instrument from Varian. A Fluorolog-322 spectrometer from Horiba Jobin-Yvon was used for steady-state luminescence spectroscopy. Time-resolved luminescence and transient absorption experiments were performed using an LP920-KS spectrometer from Edinburgh Instruments, using the frequency-doubled output of a Quantel Brilliant b laser as an excitation source.

5.2 Syntheses and product characterization data

5.2.1 Compound **7**

Following a previously published procedure [16], 1,3,5-tribromobenzene (5.00 g, 15.9 mmol) and 2-methyl-3-butyn-2-ol (3.41 ml, 34.9 mmol) were dissolved in dry triethylamine (85 ml). After de-oxygenating, CuI (4 mol-%) and $PdCl_2(PPh_3)_2$ (2 mol-%) were added, and the reaction mixture was heated to reflux under N_2 for 1 hour. Then the solution was cooled to room temperature, and ethyl acetate was added. The mixture was washed with saturated aqueous NH_4Cl and with brine. After drying over anhydrous Na_2SO_4 the solvents were evaporated. Chromatography on silica gel column occurred first with a 5:1 (v:v) and then with a 3:1 (v:v) mixture of pentane and ethyl acetate as the eluent. This afforded the product as a yellow crystalline solid (3.59 g, 11.2 mmol, 70%). ^{1}H NMR (400 MHz, $CDCl_3$): δ [ppm] = 7.49 (d, J = 1.4 Hz, 2 H), 7.40 (t, J = 1.4 Hz, 1 H), 1.98 (s, 2 H), 1.60 (s, 12 H).

5.2.2 Compound **8**

Compound **7** (3.38 g, 10.52 mmol) was dissolved in dry diethyl ether (50 ml) and cooled to -78 °C under N_2. 2.5 M *n*-BuLi in hexane (13.9 ml, 34.7 mmol) was added dropwise. Then the cooling bath was removed, and the solution was stirred for 2 hours. Prior to adding dimesitylfluoroborane (5.64 g, 21.1 mmol) in dry diethyl ether (50 ml), the reaction mixture was cooled again to -78 °C. After stirring for 10 minutes at this temperature, the cooling bath was removed, and the mixture was stirred at room temperature under N_2 overnight. Then, de-ionized H_2O was added and the phases were separated. The organic phase was dried over anhydrous Na_2SO_4 and then evaporated. The resulting brown oil was purified by chromatography on silica gel column using first pure pentane and then a 8:1 (v:v) mixture of pentane and ethyl acetate as the eluent. This afforded the product as a yellow crystalline solid (2.99 g, 6.1 mmol, 58%). ^{1}H NMR (400 MHz, $CDCl_3$): δ [ppm] = 7.59 (t, *J* = 1.7 Hz, 1 H), 7.47 (d, *J* = 1.7 H, 2 H), 6.82 (s, 4 H), 2.31 (s, 6 H), 1.96 (s, 12 H), 1.58 (s, 12 H).

5.2.3 Dialkyne **9**

Compound **8** (2.99 g, 6.1 mmol) was dissolved in dry toluene (50 ml), NaH (731 mg, 18.3 mmol) was added, and the mixture was heated to 100 °C under N_2 until completion of the reaction. (Reaction progress was monitored by thin-layer chromatography). After cooling to room temperature, the precipitate was filtered off, and the solvent was evaporated. The solid residue was purified by chromatography on a silica gel column using pentane as the eluent. This afforded the product as a pale yellow crystalline solid (0.72 g, 1.9 mmol, 31%). ^{1}H NMR (400 MHz, acetone-d_6): δ [ppm] = 7.70 (t, *J* = 1.6 Hz, 1 H), 7.59 (d, *J* = 1.6 Hz, 2 H), 6.82 (s, 4 H), 3.04 (s, 2 H), 2.31 (s, 6 H), 1.97 (s, 12 H).

5.2.4 Ligand **15**

Dialkyne compound **9** (100 mg, 0.267 mmol), iodoxylene-bpy compound **14** (103 mg, 0.267 mmol) [15], and iodo-substituted triarylamine **4** (115 mg, 0.267 mmol) [15] were dissolved in dry triethylamine (20 ml). After de-oxygenating, CuI (4 mol-%) and $PdCl_2(PPh_3)_2$ (2 mol-%) were added,

and the reaction mixture was heated to reflux under N_2 for 1 hour. Ethyl acetate was added after cooling to room temperature. The mixture was washed with saturated aqueous NH_4Cl and with brine. The organic phase was dried over anhydrous Na_2SO_4 and then evaporated to dryness. Column chromatography on silica gel occurred first with pure CH_2Cl_2 as the eluent, and then with a 100:10:1 (v:v:v) mixture of pentane, ethyl acetate and triethylamine. This afforded the pure product as a pale yellow solid (23 mg, 0.025 mmol, 9%). ^{1}H NMR (400 MHz, acetone-d_6): δ [ppm] = 8.70 (d, J = 4.1 Hz, 1 H), 8.67 (d, J = 1.7 Hz, 1 H), 8.55 (dd, J = 13.2, 8.1 Hz, 2 H), 7.99-7.90 (m, 2 H), 7.86 (s, 1 H), 7.59 (s, 1 H), 7.55 (s, 1 H), 7.49 (s, 1 H), 7.43 (dd, J = 8.0, 4.2 Hz, 1 H), 7.33 (AB_q, J_{AB} = 8.9 Hz, 2 H), 7.27 (s, 1 H), 7.11 (AB_q, J_{AB} = 9.0 Hz, 4 H), 6.94 (AB_q, J_{AB} = 9.0 Hz, 4 H), 6.90 (s, 4 H), 6.76 (AB_q, J_{AB} = 8.9 Hz, 2 H), 3.80 (s, 6 H), 2.51 (m, 4 H), 2.30 (m, 8 H), 1.97 (s, 12 H).

5.2.5 **TAA-B-Ru^{2+}** dyad

Ligand **15** (155 mg, 0.166 mmol) and $Ru(bpy)_2Cl_2$ (80 mg, 0.166 mmol) were heated to reflux in a mixture of $CHCl_3$ (5 ml) and CH_3OH (16 mmol) under N_2 overnight. Then the solvents were removed on a rotary evaporator, and purification occurred by column chromatography on a silica gel stationary phase. At first pure acetone was used as the eluent, then a 10:1 (v:v) mixture of acetone and de-ionized H_2O was employed, and finally a 100:10:1 (v:v:v) mixture of acetone, H_2O and saturated aqueous KNO_3 solution was used. The solvents were evaporated from the desired chromatography fractions, and the product was re-dissolved in CH_3CN. Excess KNO_3 was filtered off on a P4 frit. The concentrated CH_3CN solution of the product was added dropwise to a saturated aqueous KPF_6 solution. The resulting precipitate was washed with de-ionized H_2O and with diethyl ether. The pure product was obtained after drying in vacuum (130 mg, 0.074 mmol, 45%). ^{1}H NMR (400 MHz, acetone-d_6): δ [ppm] = 8.90 (dd, J = 12.3, 8.0 Hz, 3 H), 8.85 (t, J = 8.8 Hz, 4 H), 8.23-8.15 (m, 7 H), 8.11-8.07 (m, 5 H), 7.92 (d, J = 1.6 Hz, 1 H), 7.80 (t, J = 1.6 Hz, 1 H), 7.65-7.51 (m, 8 H), 7.34 (s, 1 H), 7.32 (AB_q, J_{AB} = 8.9 Hz, 2 H), 7.11 (AB_q, J_{AB} = 9.0 Hz, 4 H), 6.95 (AB_q, J_{AB} = 9.0 Hz, 4 H), 6.89 (s, 4 H), 6.75 (AB_q, J_{AB} = 8.9 Hz, 2 H), 3.80 (s, 6 H), 2.40 (s, 3 H), 2.29 (s, 6 H), 2.03 (s, 12 H), 1.97

(s, 3 H). ESI-MS (m/z): 675.1 (calc. 674.8 for $C_{86}H_{74}N_7O_2BRu^{2+}$). Anal. Calcd for $C_{86}H_{74}N_7O_2BF_{12}P_2 \cdot 4H_2O \cdot CH_3CN$: C, 60.31; H, 4.89; N, 6.39. Found: C, 60.56; H, 4.62; N, 6.26.

6. References

[1] C.R. Wade, A.E.J. Broomsgrove, S. Aldridge, F.P. Gabbaï, Chem. Rev. 110 (2010) 3958-3984.

[2] T.W. Hudnall, C.W. Chiu, F.P. Gabbaï, Acc. Chem. Res. 42 (2009) 388-397.

[3] X.Y. Liu, D.R. Bai, S.N. Wang, Angew. Chem. Int. Ed. 45 (2006) 5475-5478.

[4] C.D. Entwistle, T.B. Marder, Angew. Chem. Int. Ed. 41 (2002) 2927-2931.

[5] S. Yamaguchi, A. Wakamiya, Pure Appl. Chem. 78 (2006) 1413-1424.

[6] F. Jäkle, Coord. Chem. Rev. 250 (2006) 1107-1121.

[7] G. Zhou, M. Baumgarten, K. Müllen, J. Am. Chem. Soc. 130 (2008) 12477-12484.

[8] Z.M. Hudson, S.N. Wang, Acc. Chem. Res. 42 (2009) 1584-1596.

[9] A.G. Bonn, O.S. Wenger, J. Org. Chem. 80 (2015) 4097-4107.

[10] J. Chen, O.S. Wenger, Chem. Sci. 6 (2015) 3582-3592.

[11] Y.Q. Fang, G.S. Hanan, Synlett (2003) 852-854.

[12] D. Hanss, O.S. Wenger, Inorg. Chem. 48 (2009) 671-680.

[13] V. Hensel, A.D. Schlüter, Liebigs Ann. (1997) 303-309.

[14] C. Lambert, G. Nöll, E. Schmälzlin, K. Meerholz, C. Bräuchle, Chem. Eur. J. 4 (1998) 2129-2135.

[15] L.G. Heinz, O. Yushchenko, M. Neuburger, E. Vauthey, O.S. Wenger, J. Phys. Chem. A 119 (2015) 5676-5684.

[16] J. Liu, C.X. Yan, S.S. Li, C.Y. Wang, Y.J. Shen, Chin. J. Chem. 30 (2012) 2861-2868.

[17] J. Hankache, M. Niemi, H. Lemmetyinen, O.S. Wenger, Inorg. Chem. 51 (2012) 6333-6344.

[18] K. Sreenath, T.G. Thomas, K.R. Gopidas, Org. Lett. 13 (2011) 1134-1137.

[19] C.W. Chiu, Y. Kim, F.P. Gabbaï, J. Am. Chem. Soc. 131 (2009) 60-61.

[20] T. Noda, Y. Shirota, J. Am. Chem. Soc. 120 (1998) 9714-9715.

[21] Z. Zhang, R.M. Edkins, J. Nitsch, K. Fucke, A. Eichhorn, A. Steffen, Y. Wang, T.B. Marder, Chem. Eur. J. 21 (2015) 177-190.

[22] W. Kaim, A. Schulz, Angew. Chem. Int. Ed. 23 (1984) 615-616.

[23] C.L. Dorsey, P. Jewula, T.W. Hudnall, J.D. Hoefelmeyer, T.J. Taylor, N.R. Honesty, C.W. Chiu, M. Schulte, F.P. Gabbaï, Dalton Trans. (2008) 4442-4450.

[24] A.A. Vlček, E.S. Dodsworth, W.J. Pietro, A.B.P. Lever, Inorg. Chem. 34 (1995) 1906-1913.

[25] A. Weller, Z. Phys. Chem. 133 (1982) 93-98.

[26] S. Yamaguchi, S. Akiyama, K. Tamao, J. Am. Chem. Soc. 123 (2001) 11372-11375.

[27] A.G. Bonn, M. Neuburger, O.S. Wenger, Inorg. Chem. 53 (2014) 11075-11085.

[28] R. Stahl, C. Lambert, C. Kaiser, R. Wortmann, R. Jakober, Chem.-Eur. J. 12 (2006) 2358-2370.

[29] F. Jäkle, Chem. Rev. 110 (2010) 3985-4022.

[30] C. Hoffend, F. Schodel, M. Bolte, H.W. Lerner, M. Wagner, Chem.-Eur. J. 18 (2012) 15394-15405.

[31] Y.M. You, S.Y. Park, Adv. Mater. 20 (2008) 3820-3826.

[32] S.T. Lam, N.A.Y. Zhu, V.W.-W. Yam, Inorg. Chem. 48 (2009) 9664-9670.

[33] J. Bourson, J. Pouget, B. Valeur, J. Phys. Chem. 97 (1993) 4552-4557.

[34] A.K.C. Mengel, B. He, O.S. Wenger, J. Org. Chem. 77 (2012) 6545-6552.

[35] H.C. Schmidt, L.G. Reuter, J. Hamacek, O.S. Wenger, J. Org. Chem. 76 (2011) 9081-9085.

[36] Y. Sun, Z.M. Hudson, Y.L. Rao, S.N. Wang, Inorg. Chem. 50 (2011) 3373-3378.

[37] Q.G. Mulazzani, S. Emmi, P.G. Fuochi, M.Z. Hoffman, M. Venturi, J. Am. Chem. Soc. 100 (1978) 981-983.

[38] G.A. Heath, L.J. Yellowlees, P.S. Braterman, J. Chem. Soc., Chem. Commun. (1981) 287-289.

[39] R.A. Marcus, N. Sutin, Biochim. Biophys. Acta 811 (1985) 265-322.

[40] E.H. Yonemoto, G.B. Saupe, R.H. Schmehl, S.M. Hubig, R.L. Riley, B.L. Iverson, T.E. Mallouk, J. Am. Chem. Soc. 116 (1994) 4786-4795.

[41] J. Wiberg, L.J. Guo, K. Pettersson, D. Nilsson, T. Ljungdahl, J. Mårtensson, B. Albinsson, J. Am. Chem. Soc. 129 (2007) 155-163.

[42] V. Lloveras, J. Vidal-Gancedo, D. Ruiz-Molina, T.M. Figueira-Duarte, J.-F. Nierengarten, J. Veciana, C. Rovira, Faraday Discuss. 131 (2006) 291-305.

[43] C. Rovira, D. Ruiz-Molina, O. Elsner, J. Vidal-Gancedo, J. Bonvoisin, J.-P. Launay, J. Veciana, Chem. Eur. J. 7 (2001) 240-250.

[44] G. Nöll, M. Avola, J. Phys. Org. Chem. 19 (2006) 238-241.

Graphic and text for the table of contents

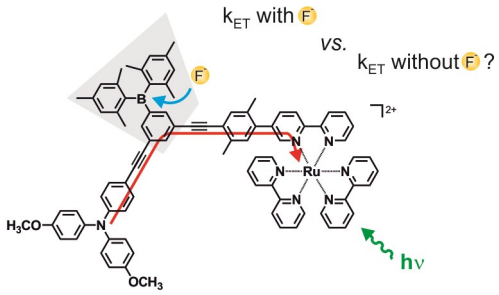

The effect of fluoride binding to an organoboron bridge on long-range electron transfer was investigated.